Assessment of reactions occurring during the solid state processing of iron-based titanium diboride composites

B. S. TERRY, O. S. CHINYAMAKOBVU*
Department of Materials, Imperial College, Exhibition Road, London SW7 2BP, UK

The reactions occurring during the solid-state processing of Fe–C/TiB$_2$ composite materials have been assessed. Optical microscopy and X-ray diffraction have been used to identify the products of reaction after sintering and hot isostatic pressing of such materials in the temperature range 1000–1200 °C. TiC has been seen to form readily at the TiB$_2$/Fe interface: an apparently continuous layer of TiC forms on the surface of the TiB$_2$, hindering further reaction. Solid state processing appears to be a potentially viable route for the production of iron-based TiB$_2$ composite materials.

1. Introduction

In a previous publication [1] we found that when both pure iron and iron–carbon liquid alloys are reacted with TiB$_2$, Fe$_2$B forms as one of the products and its brittle nature effectively precludes the viability of the liquid state processing of iron-based TiB$_2$ composites. In the work reported here, the solid state reactions between iron-based alloys and TiB$_2$ have been investigated with the aim of developing a solid state processing route for the production of iron-based TiB$_2$ composites. Pure iron, iron–carbon and iron–manganese–carbon alloys have been investigated as matrices. The latter alloys form the basis of the well-known Hadfield steels. It was hoped that the known wear resistance of these materials could be enhanced by the incorporation of TiB$_2$ filler material; a previous investigation of Fe–Mn/TiB$_2$ composites produced by hot isostatic pressing [2] produced a material with good wear properties but the analysis of the reactions occurring and phases formed during the materials production was incomplete.

The purpose of the present investigation was to assess what reactions are liable to occur during the solid state processing of iron alloy/TiB$_2$ composite materials, and thus to evaluate the potential of solid state processing routes for producing wear-resistant iron-based TiB$_2$ composites.

2. Experimental procedure

The experiments conducted in this study were as follows.

1. Metallographic and X-ray diffraction analysis of Fe–Mn/TiB$_2$ composites which had previously been isostatically hot-pressed at 1100 °C for 1 h. This pressing was performed by ESK of Germany.

2. Heat treatment and subsequent analysis of the above isostatically hot-pressed samples. These heat treatments involved levitation heating at 1600 or 1200 °C.

3. Heat treatment of mixtures of iron-alloy and TiB$_2$ mixtures in the temperature range 1100–1200 °C.

The hot isostatically-pressed samples consisted of an iron alloy matrix of composition 12 wt % Mn, 1.2–1.4 wt % C, 0.3 wt % Si, 0.1 wt % P and 0.04 wt % S, to which was added 10 wt % F 16 grade (1000–1300 μm) TiB$_2$, as a filler. All heat treatments were performed in sealed argon-filled silica tubes. The samples were then allowed to air-cool prior to removal from the silica tube.

Microhardness measurements were made on selected samples using a Lietz (miniload 2) microhardness tester with a diamond indentor and using 50 and 100 g loads.

3. Results and discussion

3.1. Heat treatment of isostatically hot-pressed samples.

Table I provides a survey of the experiments conducted and results obtained after the heat treatment of isostatically hot-pressed samples. Typical microstructures of the products of heat treatment are shown in Fig. 1.

X-ray diffraction analysis of the as-received hot isostatically pressed sample revealed the presence of TiC as one of the major constituents. Microstructural examination showed that TiC had formed round the edges of the TiB$_2$ particles (Fig. 1a) and immediately surrounding this TiC rim was a lamellar region consisting of a hard light phase (857 H$_v$) and a softer dark phase (304 H$_v$) as shown in Fig. 1b. X-ray diffraction

---

* *Present address:* Department of Metallurgical Engineering, University of Zimbabwe, Zimbabwe.

TABLE I Heat treatment of HIPed Fe, Mn–TiB$_2$ samples

| Sample	Treatment	X-ray analysis	Comments
ESK	As-received, i.e. pressed at 1100 °C, 1900 bar for 1 h	TiB$_2$, TiC, (Fe, Mn)$_{23}$ (C, B)$_6$, poss. Fe$_3$C/Mn$_5$C$_2$	The Fe lines did not show strongly but the sample responded positively to a magnetic test
ESK-HT	As above, then heat treated under argon at 1100 °C for 24 h	As above, exactly	Fe$_3$C presence evinced by pearlite presence in microstructure
ESK-LT	As in ESK sample, then levitated at 1600 °C in flowing Ar	Fe, TiB$_2$, TiC, Fe$_3$C, poss. Fe$_2$B	Manganese in solution?
ESK-LT-HT	As above (ESK-LT), then further heat treated at 1100 °C for 18 h under Ar	Fe, TiB$_2$, TiC (Fe, Mn)$_{23}$ (C, B)$_6$ poss Fe$_3$C/Mn$_5$C$_2$	The X-ray is like that for ESK above, but Fe lines now prominent and TiB$_2$ lines fainter
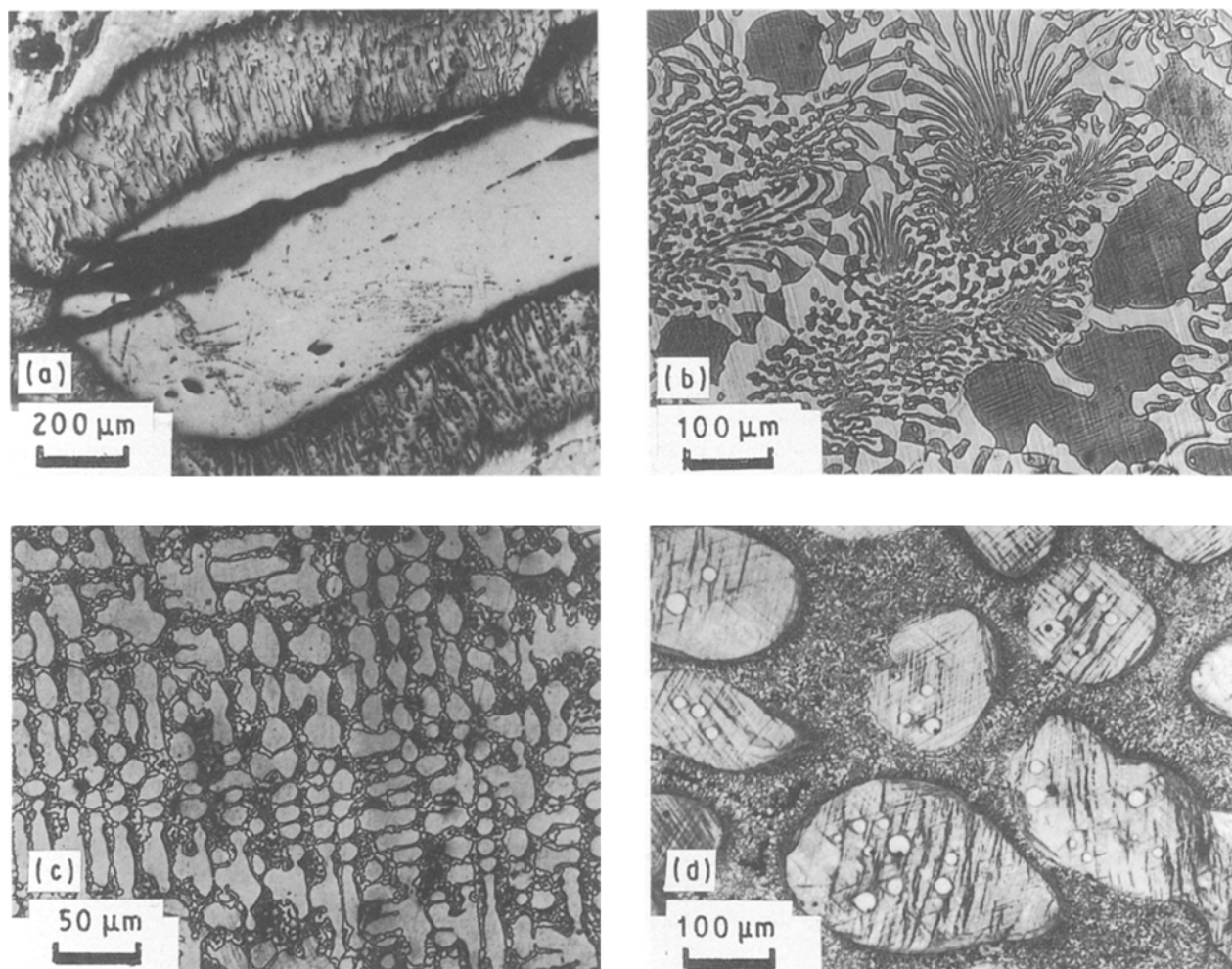
Figure 1 Microstructure observed after various heat treatments of Fe, Mn–TiB$_2$ pellets. (a) A TiB$_2$ particle surrounded by TiC in a ferromanganese matrix. Note the delamination at the TiB$_2$/TiC interface. The big crack was due to sample preparation. (b) The matrix (at high magnification) structure immediately next to the hard particles. It is believed the dark phase is ferrite and the light phase is (Fe, Mn)$_{23}$ (C, B)$_6$. (c) After levitation of HIPed Fe, Mn–TiB$_2$ samples, dendritic microstructures were observed. (d) There is a dramatic change of microstructure after heat treatment of the sample in (c). The phases identified were the same as those in (a).

revealed the presence of either M$_{23}$C$_6$ or Fe$_{23}$(C, B)$_6$. These compounds have identical structures and cell dimensions and, in fact, it is likely that the compound present was of the form (Fe, Mn)$_{23}$(C, B)$_6$. It is thought that the light phase illustrated in Fig. 1b was this iron–manganese–boro-carbide and that the darker colamaellar phase was ferrite.

It is therefore clear that pressing of Fe–C/TiB$_2$ mixtures at 1100 °C leads to the formation of TiC. A mass balance calculation indicates that total conver-

sion of TiB$_2$ to TiC in the ESK alloy would require a carbon content of 1.7% C as the initial iron matrix. As the alloy contained 1.2–1.4 wt % C it was felt that a prolonged heat treatment at 1100 °C would enhance the conversion of most of the remaining TiB$_2$ to TiC and a boron-containing phase. A 24 h treatment at 1100 °C (sample ESK-HT) produced no apparent change in microstructure. Closer examination of both samples ESK and ESK-HT indicated that there was significant delamination at the TiB$_2$/TiC interface

which had probably occurred after the hot isostatic pressing. Further reaction of the TiB_2 was therefore impossible during subsequent heat treatment as diffusion of B and C across the TiB_2/TiC interface would have been required.

A piece of the initial ESK material was melted under levitation at 1600 °C for 3 min (sample ESK-LT). The resultant microstructure is shown in Fig. 1c. The boron carbide phase was not detected after X-ray diffraction analysis of the sample but there was a very weak iron boride pattern. It therefore appears that the boron carbide phase dissolves in the iron matrix, yielding carbon and manganese in solution and iron boride as a new phase.

Further heat treatment of the levitated sample for 18 h at 1100 °C (ESK-LT-HT) produced a dramatic change in microstructure as shown in Fig. 1d. The phases identified by X-ray diffraction were, however, exactly the same as those which had been identified for the original ESK sample.

3.2. Heat treatment of iron alloy/TiB_2 mixtures

In an attempt to clarify and to understand the reactions occurring between ferromanganese alloys and TiB_2, tube furnace experiments were performed on 1–2 g pressed powder samples with varying matrix compositions and nominally 10 wt % TiB_2 additions.

Carbonyl iron powder was used in all cases and iron–manganese samples were made by mixing it with a ferromanganese powder. Graphite powder was used as a source of carbon. The results obtained from various heat treatments are shown in Table II and typical microstructures of resultant products in Fig. 2. In Table II the term "alloy" denotes a matrix composition of Fe–12 wt % Mn, 1.2 wt % C.

In a previous study it was noted that both pure iron and iron–carbon alloys reacted with TiB_2 to form Fe_2B as one of the products after levitation melting at 1600 °C. Experiment 20X of the present study was the only one to show formation of Fe_2B at the lower temperature of 1100 °C. This was in contrast to experiments 24X and 27X which did not show any formation of Fe_2B. It is thought that the presence of graphite in these runs inhibited iron boride formation in favour of carbide or boro-carbide.

In experiment 21X the same composition was used as in the ESK hot-pressing operations and the same phases were identified. The $M_{23}X_6$ (M = Fe/Mn, X = Co/B) phase appeared to form quite readily in the presence of manganese. The phase was present after only 2 h at 1100 °C in experiment 21X and after only 1 h at 1200 °C in experiment 26X. It was also present in experiment 25X after only 2 h at 1000 °C. Short-time experiments in the absence of manganese (e.g. 24X) did not lead to the formation of the $M_{23}X_6$ phase. Longer times, however, such as 16 h in experiment 27X, did lead to the formation of the $Fe_{23}(C, B)_6$ phase and it can therefore be concluded that the presence of manganese favours and speeds up the formation of the $M_{23}X_6$ phase.

In their review of the iron-rich portion of the Fe–B–C system, Raghavan and Ghosh [3] noted that a ternary compound I with the formula $Fe_{23}(C, B)_6$ had been established in the system. The structure of I is complex cubic of the $Cr_{23}C_6$ type. They noted that similar ternary compounds could be formed by partial

TABLE II Results of low-temperature pressed-powder pellets of Fe–Mn + TiB_2 experiments

Sample	Composition	Temperature (°C)	Time/hr (h)	Phases identified XRD
20X	Pure iron TiB_2 (F 600)[a] 10 wt %	1100	17	Fe, Fe_2B, TiB_2
21X	Alloy TiB_2 (F 150)[a] 10 wt %	1100	2	Fe, TiB_2, TiC (Fe, Mn)$_{23}$ (C, B)$_6$, poss. Fe_3C
22X	Alloy TiB_2 (F 150) 26 wt %	1100	22	Fe, TiB_2 (weak) TiC (weak) (Fe, Mn)$_{23}$ (C, B)$_6$
23X	Alloy only	1100	1	Fe, Fe_3C (very weak)
24X (no Mn)	Pure Fe 94.4 wt % Graphite 1.5 wt % TiB_2 (F 150) 4.1 wt %	1100	1	Fe, TiB_2, TiC (weak) poss. Fe_3C
25X	Alloy TiB_2 (F 150) 10 wt %	1000	2	Fe, TiB_2, TiC (very weak) (Fe, Mn)$_{23}$ (C, B)$_6$, poss. Fe_3C
26X	Alloy TiB_2 (F 150) 10 wt %	1200	1	Fe, TiB_2, TiC (Fe, Mn)$_{23}$ (C, B)$_6$, Fe_3C
27X (no Mn)	Pure iron 89 wt % Graphite 1.6 wt % TiB_2 (F 150) 8.9 wt %	1100	16	Fe, TiB_2, TiC, Fe_{23} (C, B)$_6$

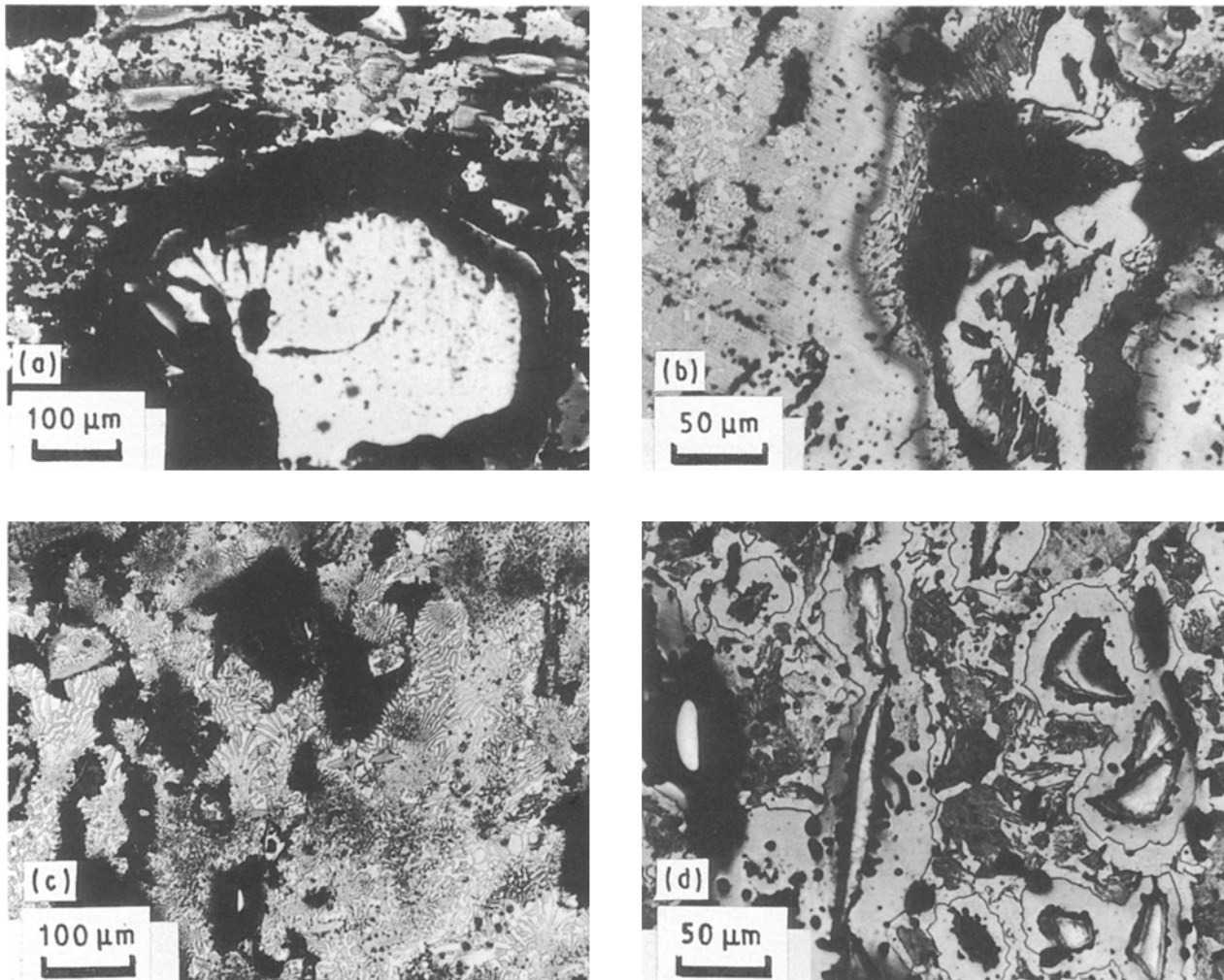[a] F 600 10 μm and under; F 150 70–100 μm.

Figure 2 Microstructures observed after sintering Fe–Mn–TiB$_2$ pellets in a tube furnace. (a) A large TiB$_2$ particle is surrounded by a region of delamination. (b) Microstructure of sintered Fe, Mn alloy with no TiB$_2$. (c) The commonly observed Fe/(Fe, Mn)$_{23}$ (C, B)$_6$ lamella pattern is clearly illustrated. (d) The matrix is predominantly pearlitic, but only ferritic regions surround the hard TiB$_2$/TiC particles.

substitution of the iron by molybdenum or tungsten. The work reported here indicates that manganese can also substitute for iron. The stability range of I has been reported to be between a possible lower limit of 600 °C and an upper limit of 965 °C [3]. This would suggest that the M$_{23}$X$_6$ phase observed after performing experiments at 1000 °C and above in the present study was only found during cooling. Samples air-quenched from 1100 °C (e.g. ESK-HT) however, still showed a strong presence of this phase, indicating that the presence of manganese may increase the temperature range over which the M$_{23}$X$_6$ phase is stable.

Experiments at 1000 and 1200 °C (25X and 26X, respectively) differed only in that at the lower temperature the TiC pattern was much weaker, but all the other phases were still present. The use of lower processing temperatures therefore appears to reduce the extent of conversion of TiB$_2$ to TiC.

3.3. Prospects for Fe/TiB$_2$ composite production

It appears clear from the present study that the formation of Fe$_2$B can be prevented during the solid state

processing of the Fe–TiB$_2$ and Fe–Mn/TiB$_2$ composite materials. TiC formation can occur to varying extents, depending on processing conditions. The TiC formed is produced at the iron/TiB$_2$ interface. Its subsequent influence on composite properties is not clear at this stage, and a detailed study is required in this area.

It is encouraging, however, that wear-testing of Fe–Mn/TiB$_2$ [2] composites, produced by hot isostatic pressing, has produced results superior to those of cast iron, manganese steel and alumina. It is, however, difficult to envisage hot isostatic pressing as an economical route to producing such materials and there is a clear need for a cheaper solid state processing route. Sintering, followed by hot pressing or forging may provide a way forward. The delamination observed at the TiB$_2$/TiC interface during the present study may very well be detrimental to material properties and therefore further examination of the effects of processing conditions on the extent of such delamination is required.

Eutectic material produced by the reaction of TiB$_2$ and TiC has recently been reported to have properties superior to both TiB$_2$ and TiC in relation to its use as a filler material. Its lower melting point is also liable to

make its production easier and less expensive than the pure components. The incorporation of such eutectic material into iron matrices by a number of means is now being investigated.

4. Conclusions

1. Formation of Fe_2B can be avoided during the solid state processing of iron-based TiB_2 composite materials.

2. TiC formation readily occurs when the iron matrix contains dissolved carbon.

3. The TiC forms as an apparently continuous layer at the surface of the TiB_2.

4. Solid state processing appears to be a potentially viable route for the production of Fe/TiB_2 composite materials.

References

1. B. S. TERRY and O. S. CHINYAMAKOBVU, *Mater. Sci. Technol.*, in press.
2. V. ADEY and I. C. ALEXANDER, in "Antiwear '88" (The Institute of Metals, London, 1988) pp. 102–112.
3. V. RAGHAVAN and G. GHOSH, *J. Alloy Phase Diagrams* 2(2) (1986) 77.
4. H. HOLLECK *Int. J. Refract. Hard Metals* (1987) 149.